Journal of Innovative Optical Health Sciences
Vol. 12, No. 1 (2019) 1840002 (8 pages)

DOI: 10.1142/S1793545818400023

World Scientific
www.worldscientific.com

Arbitrary amplitude femtosecond pulse shaping via a digital micromirror device

Chenglin Gu*,†, Dapeng Zhang†, Yina Chang† and Shih-Chi Chen†,‡
*State Key Laboratory of Precision Spectroscopy
East China Normal University
Shanghai 200062, P. R. China
†Department of Mechanical and Automation Engineering
The Chinese University of Hong Kong, Shatin, N.T.
Hong Kong SAR, P. R. China
‡scchen@mae.cuhk.edu.hk

Received 8 August 2018
Accepted 28 October 2018
Published 21 November 2018

An ultrafast spectrum programmable femtosecond laser may enhance the performance of a wide variety of scientific applications, e.g., multi-photon imaging. In this paper, we report a digital micromirror device (DMD)-based ultrafast pulse shaper, i.e., DUPS, for femtosecond laser arbitrary amplitude shaping — the first time a programmable binary device reported to shape the amplitudes of ultrafast pulses spectrum at up to 32 kHz rate over a broad wavelength range. The DUPS is highly efficient, compact, and low cost based on the use of a DMD in combination with a transmission grating. Spatial and temporal dispersion introduced by the DUPS is compensated by a quasi-4-f setup and a grating pair, respectively. Femtosecond pulses with arbitrary spectrum shapes, including rectangular, sawtooth, triangular, double-pulse, and exponential profile, have been demonstrated in our experiments. A feedback operation process is implemented in the DUPS to ensure a robust and repeatable shaping process. The total efficiency of the DUPS for amplitude shaping is measured to be 27%.

Keywords: Spectrum shaping; ultrafast laser; digital micromirror device.

1. Introduction

Programmable ultrafast optical pulse shapers have wide applications ranging from basic dispersion control to custom-shaped laser pulses for controlling the motion of quantum states,[1] photochemical reactions,[2] etc. Spectrum amplitude shaping is particularly important in ultrafast pulse shaping due to its broad scientific and industrial applications. For example, they are frequently used in

‡Corresponding author.

communication systems,[3,4] coherent control and biomedical imaging,[5] laser amplifiers for pre-shaping the seed lasers,[6] and oscillators with pulses of designed spectrum.[7] Programmable shaping of ultrafast pulses based on waveform synthesis is achieved by spatial modulation of the spatially dispersed optical frequency spectrum — an effective approach that is both robust and commercially available. The key element is a spatial light modulator, which can be a liquid crystal spatial light modulator (LC-SLM),[8,9] acousto-optic modulators (AOM),[10] or micro-electro-mechanical systems (MEMS)-based device.[11,12] Although LC-SLMs are efficient (60–80%), their low switching rate ($\sim$10 s Hz) and restricted wavelength range (typically 400–1700 nm) limit further applications. For example, an LC-SLM does not work ideally with aromatic rings, excited in 250 $\sim$ 400 nm.[13] For the AOM, although it has an update rate of 100s kHz, synchronization between the AOM and laser source is always required due to its operating principle, i.e., modulation of pulses via acoustic waves. Accordingly, AOM-based pulse shapers only work for lasers of a repetition rate equal to or lower than its update rate. MEMS-based pulse shapers[14] have the advantages of broadband reflectivity, high efficiency, and fast update rate (up to kHz), but their spectral resolution is relatively low (approximately tens of pixels). This technology continues to evolve in spite of the high cost. Recently, digital micromirror devices (DMDs) have been used for pulse shaping,[15,16] i.e., phase shaping, achieving high update rate (2 MHz) with a limited efficiency (1.7%).

In this paper, we present a DMD-based ultrafast pulse shaper, i.e., DUPS, the first binary pulse shaper achieving arbitrary spectrum amplitude shaping with an efficiency of 27%. The DMD consists of a large array of binary microscopic mirrors that can be operated at high speeds (4–32 kHz). Since its introduction in 1996, DMDs have been proved to be an excellent optical device in a variety of applications, such as spectral imaging,[17] spatial beam mode shaping,[18,19] adaptive optics,[20] terahertz application,[21] 3-D random-access multiphoton imaging,[22] etc. DMDs present particular strength in ultrafast pulse shaping for the following reasons: (1) low cost (versus LC-SLM and AOM); (2) high frame rate, thus high shaping rate; (3) broad bandwidth: coatings from 400 nm to 2500 nm are commercially available with the possibility to be extended to ultraviolet range; (4) high damage threshold: the damage threshold of the DMD is equal to mirrors of the same optical coating; and (5) high efficiency: the high fill factor ($\sim$92%) and switching cycle make it an effective SLM, e.g., 86% efficiency can be achieved in visible wavelength. The DUPS utilizes the DMD for arbitrary spectrum amplitude shaping. As shown in Fig. 1, the system is designed based on a quasi-4-f setup, in which the spectrum of the beam is shaped by the DMD. A grating pair (T-1200-850-2216-94, Lightsmyth) is introduced after the beam expander to compensate the dispersion introduced by the quasi-4-f configuration. In the following sections, we will demonstrate arbitrary spectrum shaping for the selected spectrum shapes, including rectangular, sawtooth, triangular, and exponential profiles. The overall efficiency of the DUPS is measured to be 27%, and the shaping rate is equal to the update rate of the DMD.

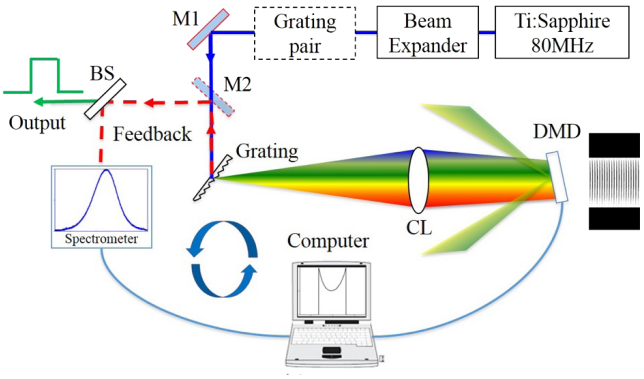

Fig. 1. Experimental setup of the DUPS. M1-M2: high-reflection mirrors; BS: beam splitter; CL: cylindrical lens; DMD: digital micromirror device.

2. Experiment

Figure 1 presents the optical configuration and the experimental procedure. The laser source is a Ti: Sapphire ultrafast oscillator (Chameleon Ultra II, Coherent, USA) with an average power of 4 W, pulse width of $\sim$200 fs, and repetition rate of 80 MHz at 800 nm. The oscillator has an output beam diameter of $\sim$ 1 mm. After being resized to 3 mm via the beam expander, the beam undergoes a transmission grating that disperses the spectrum spatially. The grating has a groove density of 1200 lines/mm and an efficiency of 90%. After that, the spectrum is projected to the DMD

(DLP4500NIR, Texas Instrument 0.45 Inch, 1140 × 912 pixels) by a cylindrical lens with a focal length of 400 mm. The diffracted beam is aligned to be collinear with the incident beam when micromirrors on the DMD are 12° tilted. The grating then recombines the spatially dispersed spectrum to form an ultrafast pulse. The DMD is also slightly tilted downward to separate the diffracted beam for guiding it to the spectrometer (resolution = 0.3 nm) by M2 and the beam splitter. Next, the computer calculates new patterns on the DMD based on the measured spectrum data to refine the shape of the spectrum amplitude. This feedback strategy ensures that the result is accurate and reliable. From the experiments, we find that one loop is enough to achieve the desired spectrum shape.

The quasi-4-f arrangement is different from typical 4-f systems for pulse shaping because the nonzero (-5th) diffraction order of the DMD is used. Under this condition, the DMD becomes equivalent to a blazed grating of a groove density of 463 lines/mm at the first-order diffraction. The DMD can be seen as a cylindrical mirror with a focal length $f_{\mathrm{DMD}} = \pm\frac{f_{\mathrm{cyl}} d_g \cos\theta}{d_d \cos\beta}$, where f_{DMD} is the equivalent focal length of the DMD for the spectrum; the sign is determined by the blazing direction between (transmission) grating and the DMD; f_{cyl} is the focal length of the cylindrical lens; θ is the diffraction angle of the grating; β is the diffraction angle of the DMD; d_g is the groove density of the grating; and d_d is the equivalent groove density of the DMD (463 lines/mm in our experiment). To image the spectrum to the DMD precisely, the distance between the cylindrical lens and the DMD is f_{cyl}. The distance (l) between grating and the cylindrical lens is adjusted to ensure that the diffracted monochromatic beams and the incident beam are collinear. l is calculated to be

$$l = f_{\mathrm{cyl}} - \frac{f_{\mathrm{cyl}}^2}{2f_{\mathrm{DMD}}}. \tag{1}$$

It has been established that group velocity dispersion (GVD) will be introduced when a spatially dispersed pulse encounters a grating or prism.[23,24] Since the DMD functions like a grating in the DUPS, it introduces additional GVD to ultrafast pulses. The DUPS introduces both spatial and temporal dispersion. Spatial dispersion is caused by the angular dispersion of the spectrum, i.e., spatial dispersion is introduced when the laser beam is focussed or defocussed by the DMD. At first, a blazed grating spatially disperses the spectrum of a pulse. The first-order angular dispersion of the grating is:

$$\frac{d\lambda}{d\theta} = \frac{d}{m}\cos\theta, \tag{2}$$

where m is the diffraction order and d is the grating period. The spatial dispersion on hologram is

$$\frac{d\lambda}{dx} = \frac{d\lambda}{d\theta}\frac{d\theta}{dx} = \frac{d\cos\theta}{mf_{\mathrm{cyl}}}, \tag{3}$$

where f_{cyl} is the focal length of the cylindrical lens and λ is the center wavelength of the pulse. For example, when using a grating of 1200 lines/mm, $f_{\mathrm{cyl}} = 400$ mm, $\lambda = 750$ nm, and $d\lambda/dx = 1.68$ nm/mm. In the angular frequency (ω) domain:

$$\alpha = \frac{dx}{d\omega} = \frac{dx}{d\lambda}\frac{d\lambda}{d\omega} = -\frac{2\pi \mathrm{cmf}_{\mathrm{cyl}}}{d\cos\theta\omega^2}. \tag{4}$$

As the DMD functions as a cylindrical lens to the spectrum, the parabolic phase introduced by the DMD is equivalent to that introduced by a cylindrical mirror in the spectral plane:

$$\varphi = -ik\frac{\alpha^2\omega^2}{2f_{\mathrm{DMD}}}. \tag{5}$$

The GVD β_2 is the second derivative of φ with respect to ω:

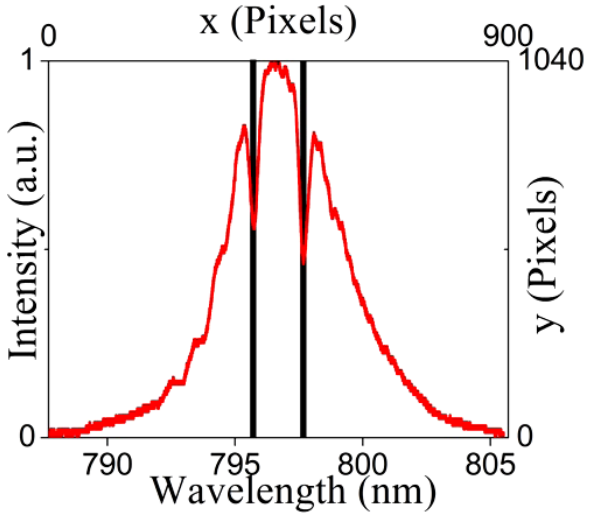

Fig. 2. (Color online) Calibration of the DUPS with Cartesian coordinate system defined on the DMD; red curve: spectrum with modulation; black stripes: pattern with corresponding "off" pixels on the DMD.

$$\beta_{21} = -\frac{8\pi^2 c}{d^2 \cos^2\theta \omega^3} \frac{f_{\text{cyl}}^2}{2f_{\text{DMD}}}. \tag{6}$$

The temporal dispersion is caused by the nonlinearity of the angular frequency distribution on the DMD:

$$\beta_{22} = \frac{16 \sin\theta \pi^2 c}{d^2 \cos^3\theta \omega^3} \tan\beta f_{\text{cyl}}. \tag{7}$$

The absolute value of β_{22} is equal to the GVD introduced by a pair of gratings with a period d and $2\sin\theta\tan\beta f_{\text{cyl}}$ apart. The total GVD of the DUPS is the sum of Eqs. (6) and (7):

$$\beta_2 = -\frac{8\pi^2 c}{d^2 \cos^2\theta \omega^3} \frac{f_{\text{cy}}^2}{2f_{\text{DMD}}} + \frac{16 \sin\theta \pi^2 c}{d^2 \cos^3\theta \omega^3} \tan\beta f_{\text{cyl}}. \tag{8}$$

Since the angular dispersion of GVD is already compensated by setting the grating and the cylindrical lens out of focus, there is only β_{22} left in the DUPS.

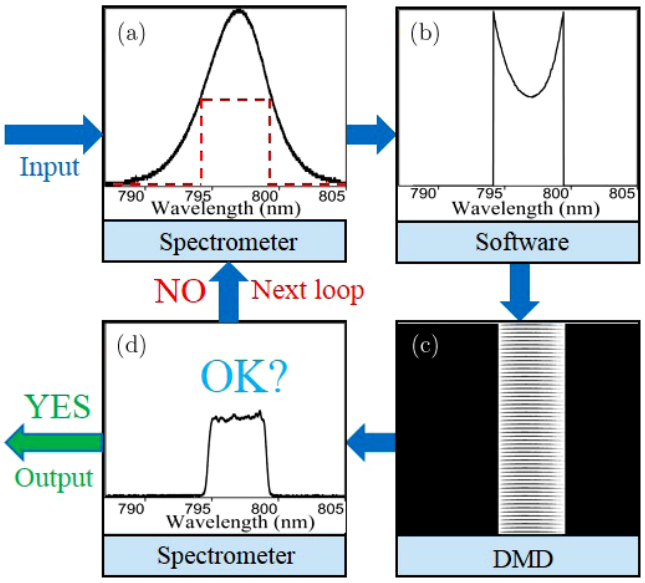

Fig. 3. (Color online) (a) Measured spectrum of an input pulse (black curve) and target spectrum (red curve); (b) shaping function calculated by the computer; (c) patterns for spectrum shaping on the DMD; and (d) shaped spectrum.

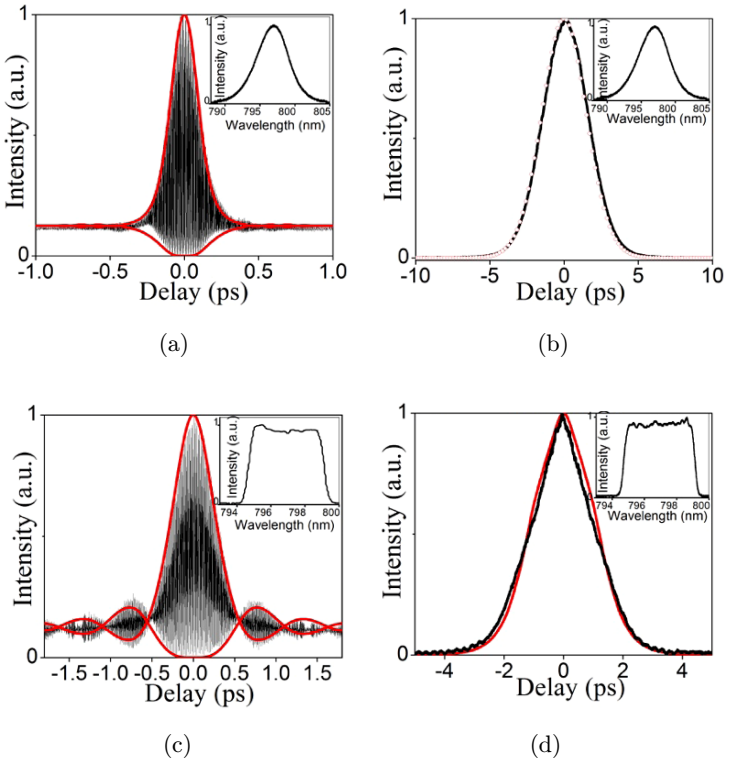

Fig. 4. (Color online) (a) and (b) Autocorrelation curves of output pulses with and without the dispersion compensation, respectively (no modulation on DMD). Black curve: experimental curves; red curve: theoretical curves. Inset: initial spectrum. (c) and (d) Autocorrelation curves of output pulses with and without the dispersion compensation, respectively (rectangle modulation on DMD). Black curve: experimental curves; red curve: theoretical curves. Inset: spectrum of the shaped pulses.

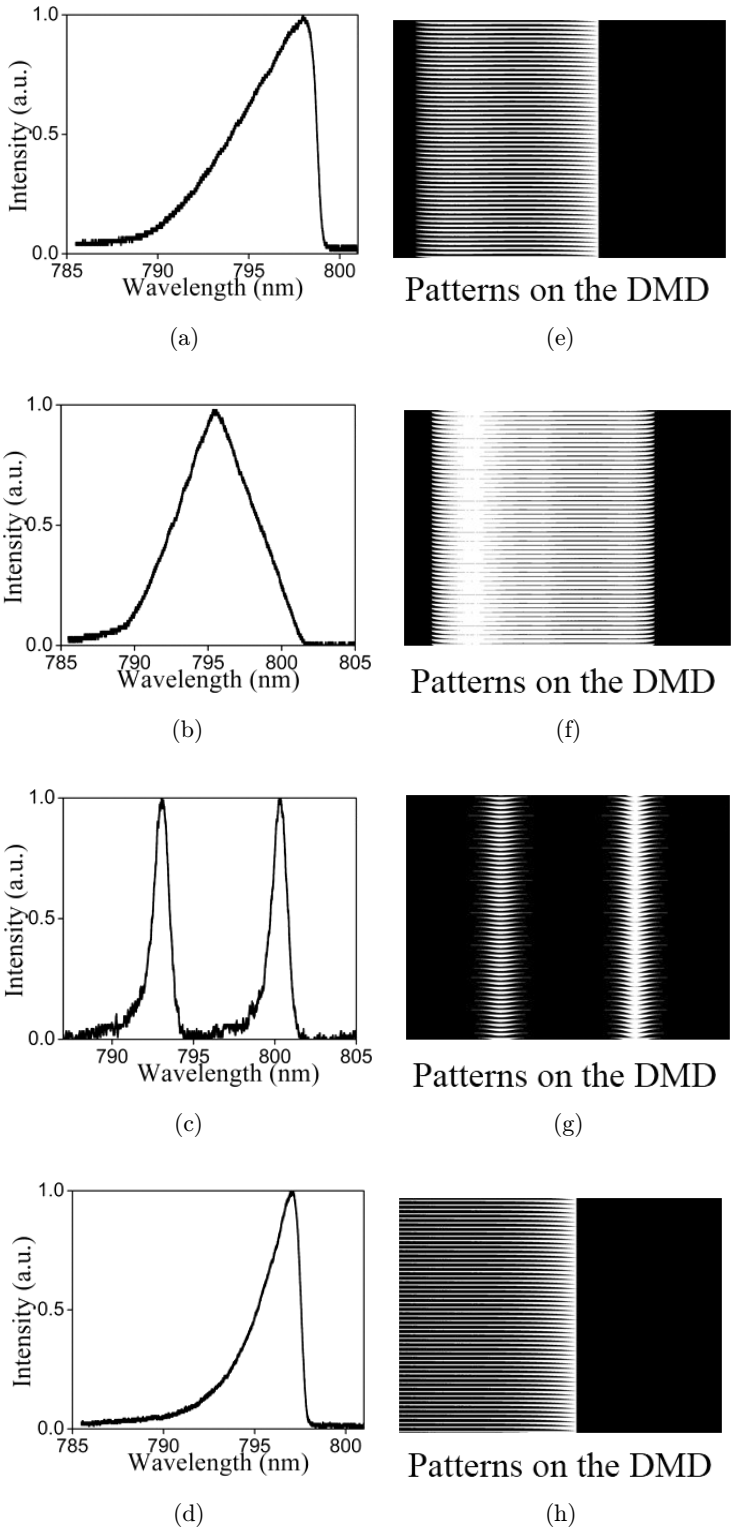

Fig. 5. (a)–(d) Shaped spectra with sawtooth, triangular, double-pulse, and exponential profiles, respectively; (e)–(h) corresponding patterns on the DMD.

3. Results and Discussion

In this section, we present experimental results of arbitrary spectrum amplitude shaping. Before the experiments, we first calibrate the system, i.e., the distribution of a spectrum on the DMD, through a spectrometer, in which we assume that the spectrum is dispersed along the x direction (horizontal direction) of the DMD. Then, we program two "black stripes" separated by 100 pixels on the DMD to block two individual spectra as shown in Fig. 2. (Note that the top and right edges of Fig. 2 are labeled with the coordinate system on the DMD as well as the number of total pixels in each direction). Accordingly, from the spectrometer, we find two corresponding notches at 795.8 nm and 797.7 nm in the spectrum, as shown in Fig. 2. The spectrum distribution $\lambda(x)$ on the DMD is then calculated to be 0.019 nm/pixel, equivalent to 1.76 nm/mm, and the wavelength in the center of the DMD is 796.7 nm:

$$\lambda(x) = 796.7 + 1.76x. \tag{9}$$

Arbitrary amplitude shaping is achieved by controlling the diffraction property of the grating with rectangular groove profile. Gratings-like patterns with varying duty cycles along x direction are programmed on the DMD. The duty cycle $D(x) = a(x)/\gamma(x)$ can be written as a function of x, where a is the width of the stripe and γ is the period of the grating. The zero-order diffraction efficiency is the square of the duty cycle:

$$\eta(x) = D^2(x). \tag{10}$$

From Eqs. (9) and (10), we can obtain the shaping function:

$$M(\lambda) = D^2(0.57\lambda - 452.7). \tag{11}$$

An amplitude shaping experiment is first conducted to validate the DUPS without the grating pair for dispersion compensation. As shown in Fig. 3(a), a femtosecond pulse is first sent to the DUPS, in which the spectrum is measured for calculating the required modulation function, as shown in Fig. 3(b). After obtaining the modulation function via Eq. (11), the corresponding patterns on the DMD are calculated based on Eq. (10), and the target spectrum amplitude is achieved. The grating pattern on the DMD has a period of 140 μm (23 pixels). The feedback loop can be repeated to achieve better precision. The final rectangle spectrum is shown in Fig. 3(d).

Next, we demonstrate arbitrary amplitude modulation with a grating pair for compensating the GVD introduced by the DUPS, where the grating pair is placed 6.6 cm apart calculated from Eq. (7). The experimental results are shown in Fig. 4. Figure 4(a) shows the autocorrelation curves of the output pulses without modulation ("white" screen on the DMD with a compensating grating pair), and Fig. 4(b) shows the autocorrelation curves without the grating pair; the system setup is shown in Fig. 1. Assuming the input pulses have a Gaussian profile, the duration of the output pulses with and without the compensating grating pair is 185 fs and 2.3 ps, respectively. The GVD compensated by the grating pair is about $-184{,}200\,\text{fs}^2$ The theoretical GVD introduced by the system is $200\,300\,\text{fs}^2$ according to Eq. (6). The autocorrelation curves of the modulated pulses with rectangular spectrum are shown in Figs. 4(c) and 4(d), respectively, in which the experimental results show good consistency with theoretical calculations. To validate the effectiveness of the DUPS in arbitrary amplitude shaping, some typical spectra are shaped in the following experiments. Figures 5(a)–5(d) show the shaped spectra with sawtooth, triangular, double-pulse, and exponential profiles. The corresponding patterns on the DMD are shown in Figs. 5(e)–5(h).

The efficiency of the DUPS for amplitude shaping is defined by the energy ratio of the output pulse to the input pulse with a "white" screen on the DMD. The efficiency of the transmission grating at 800 nm is ~90%, which is lower than the efficiency (94%) at its designed wavelength of 850 nm. The diffraction efficiency of the DMD is about 50%. The overall efficiency of the DUPS is ~ 40% without a pre-compressed grating pair. Given that the efficiency of the grating pair is 67%, the overall efficiency of the DUPS with pre-compression is 27%.

4. Conclusion

We have presented a DMD-based ultrafast pulse shaper, i.e., DUPS, with both theoretical analysis and experimental results, achieving arbitrary spectrum amplitude shaping with 27% efficiency for the first time. The setup of the DUPS is compact, consisting of three key components: a transmission gating, a cylindrical lens, and a DMD. The DUPS can shape an ultrafast pulsed laser at a rate that is equal to the update rate of a DMD (up to 32 kHz)

over a broad wavelength range. Spatial and temporal dispersion introduced by the DUPS is analyzed and compensated by a quasi-4-f setup and a grating pair, respectively. In addition, the feedback operation strategy enables a fast, robust, and repeatable shaping process. Femtosecond pulses with arbitrary spectrum shapes including rectangular, sawtooth, triangular, double-pulse, and exponential profiles have been demonstrated in our experiments. In the future, given the superior pixel count and constantly improving performance of the DMDs, the new shaping technique has the potential to be integrated with other scanning/shaping methods to achieve simultaneous phase and amplitude modulation of ultrafast laser pulses at higher rates.

Acknowledgment

This work is partially supported by the HKSAR Innovation and Technology Commission (ITC) Innovation and Technology Fund (ITF), ITS/179/16FP, as well as the HKSAR Research Grants Council, General Research Fund, Project No. 14202815.

References

1. J. Möhring, T. Buckup, M. Motzkus, "A quantum control spectroscopy approach by direct UV femtosecond pulse shaping," *IEEE J. Sel. Top. Quant. Electron.* **18**(1), 449–459 (2012).
2. A. Assion, T. Baumert, M. Bergt, T. Brixner, B. Kiefer, V. Seyfried, G. Gerber, "Control of chemical reactions by feedback-optimized phase-shaped femtosecond laser pulses," *Science* **282** (5390), 919–922 (1998).
3. J. Schröder, M. A. Roelens, L. B. Du, A. J. Lowery, S. Frisken, B. J. Eggleton, "An optical FPGA: Reconfigurable simultaneous multi-output spectral pulse-shaping for linear optical processing," *Opt. Expr.* **21**(1), 690–697 (2013).
4. F. Zhang, X. Ge, S. Pan, J. Yao, "Photonic generation of pulsed microwave signals with tunable frequency and phase based on spectral-shaping and frequency-to-time mapping," *Opt. Lett.* **38**(20), 4256–4259 (2013).
5. J. M. Dela Cruz, V. V. Lozovoy, M. Dantus. "Coherent control improves biomedical imaging with ultrashort shaped pulses," *J. Photochem. Photobiol. A Chem.* **180**(3), 307–313 (2006).
6. D. N. Schimpf, J. Limpert, A. Tünnermann, "Controlling the influence of SPM in fiber-based chirped-pulse amplification systems by using an actively shaped parabolic spectrum," *Opt. Expr.* **15**(25), 16945–16953 (2007).
7. S. Boscolo, C. Finot, H. Karakuzu, P. Petropoulos, "Pulse shaping in mode-locked fiber lasers by in-cavity spectral filter," *Opt. Lett.* **39**(3), 438–441 (2014).
8. A. M. Weiner, "Femtosecond pulse shaping using spatial light modulators," *Rev. Sci. Instrum.* **71**(5), 1929–1960 (2000).
9. C. Dorrer, S. K.-H. Wei, P. Leung, M. Vargas, K. Wegman, J. Boulé, Z. Zhao, K. L. Marshall, S. H. Chen, "High-damage-threshold static laser beam shaping using optically patterned liquid-crystal devices," *Opt. Lett.* **36**(20), 4035–4037 (2011).
10. C. W. Hillegas, J. X. Tull, D. Goswami, D. Strickland, W. S. Warren, "Femtosecond laser pulse shaping by use of microsecond radio-frequency pulses," *Opt. Lett.* **19**(10), 737–739 (1994).
11. S. M. Weber, J. Extermann, L. Bonacina, W. Noell, D. Kiselev, S. Waldis, J. P. Wolf, "Ultraviolet and near-infrared femtosecond temporal pulse shaping with a new high-aspect-ratio one-dimensional micromirror array," *Opt. Lett.* **35**(18), 3102–3104 (2010).
12. J. Extermann, S. M. Weber, D. Kiselev, L. Bonacina, S. Lani, F. Jutzi, J. P. Wolf, "Spectral phase, amplitude, and spatial modulation from ultraviolet to infrared with a reflective MEMS pulse shaper," *Opt. Expr.* **19**(8), 7580–7586 (2011).
13. M. Greenfield, S. D. McGrane, D. S. Moore, "Control of cis-stilbene photochemistry using shaped ultraviolet pulses," *J. Phys. Chem. A* **113**(11), 2333–2339 (2009).
14. M. Hacker, G. Stobrawa, R. Sauerbrey, T. Buckup, M. Motzkus, M. Wildenhain, A. Gehner, "Micromirror SLM for femtosecond pulse shaping in the ultraviolet," *Appl. Phys. B* **76**(6), 711–714 (2003).
15. C. Gu, D. Zhang, Y. Chang, S. C. Chen, "Digital micromirror device-based ultrafast pulse shaping for femtosecond laser," *Opt. Lett.* **40**(12), 2870–2873 (2015).
16. C. Gu, Y. Chang, D. Zhang, J. Cheng, S. C. Chen, "Femtosecond laser pulse shaping at megahertz rate via a digital micromirror device," *Opt. Lett.* **40**, 4018–4021 (2015).
17. Y. Wu, I. O. Mirza, G. R. Arce, D. W. Prather, "Development of a digital-micromirror-device-based multishot snapshot spectral imaging system," *Opt. Lett.* **36**(14), 2692–2694 (2011).
18. M. A. Preciado, K. Dholakia, M. Mazilu, "Generation of attenuation-compensating Airy beams," *Opt. Lett.* **39**(16), 4950–4953 (2014).
19. J. Cheng, C. Gu, D. Zhang, S. C. Chen, "High-speed femtosecond laser beam shaping based on binary

holography using a digital micromirror device," *Opt. Lett.* **40**(21), 4875–4878 (2015).
20. D. B. Conkey, A. M. Caravaca-Aguirre, R. Piestun, "High-speed scattering medium characterization with application to focusing light through turbid media," *Opt. Expr.* **20**(2), 1733–1740 (2012).
21. K. Murate, M. J. Roshtkhari, X. Ropagnol, F. Blanchard, "Adaptive spatiotemporal optical pulse front tilt using a digital micromirror device and its terahertz application," *Opt. Lett.* **43**(9), 2090–2093 (2018).
22. Q. Geng, C. Gu, J. Cheng, S. C. Chen, "Digital micromirror device-based two-photon microscopy for three-dimensional and random-access imaging," *Optica* **4**(6), 674–677 (2017).
23. J. D. McMullen, "Analysis of compression of frequency chirped optical pulses by a strongly dispersive grating pair," *Appl. Opt.* **18**(5), 737–741 (1979).
24. J. D. Kafka, T. Baer, "Prism-pair dispersive delay lines in optical pulse compression," *Opt. Lett.* **12**(6), 401–403 (1987).